Commun. Theor. Phys. (Beijing, China) **50** (2008) pp. 193–196

Vol. 50, No. 1, July 15, 2008

Influence of Ground State Spin of Projectile-Target on Fission Anisotropies

O.N. Ghodsi[1] and A.N. Behkami[2]

[1]Physics Department, Mazandaran University, Babolsar, Iran

[2]Physics Department, Fars Science and Research, Islamic Azad University, Iran

(Received July 12, 2006; Revised October 18, 2006)

Abstract *Fission fragment anisotropies have been investigated for various systems produced in heavy-ion reactions at near and sub-barrier energies. In particular, special attention has been paid to the entrance channel dependence of fragment angular anisotropies. The results of our analysis of the fragment angular anisotropies induced by boron, carbon, and oxygen ions on Thorium and Neptunium targets as well as Fluorine ions on Neptunium target indicate strong dependence of fragment anisotropies on the channel spin, in consistence with the predication of the pre-equilibrium model.*

PACS numbers: 21., 21.60.-n
Key words: influence of spin in heavy-ion reactions

1 Introduction

At bombarding energies sufficiently above the fission barrier the transition state model[1] is quite successful in accounting for measured angular distributions. In this model the distribution of K-states for fissioning systems is determined by the moment of inertia at fission saddle point and the nuclear temperature T.

In recent years there has been much interest in the failure of the transition state model of fission fragment angular distribution in sub-barrier heavy-ion reactions involving actinide nuclide targets. Anomalously large anisotropies around the fission barrier energies were reported in heavy-ion induced fission reactions involving actinide targets.[1,2] A recent observation of the strong influence of the ground state spin of the target on the fission fragment anisotropies in heavy-ion induced fusion fission reactions around the Coulomb barrier has attracted considerable interest.[3] In a more recent work,[4] it has been shown that the projectile spin also strongly influences the anisotropies at near barrier bombarding energies. Further investigations have confirmed that the presence of projectile and target ground state spins affects the fission fragment anisotropies in a significant way at near barrier and sub-barrier energies. We have investigated the fission fragment anisotropies for various systems at near barrier and sub-barrier energies. We have shown that the entrance channel-dependent K-state model incorporating the ground state spin of the target and projectile explains the measured fragment systems anisotropies reasonably well for systems under investigation. Our result supports the observation that the ground state spin of the target and/or projectile affects the fission fragment anisotropies of actinide system in the sub-barrier energy region.

In Sec. 2 a brief theory will be discussed. In Sec. 3 an actual calculational procedure will be presented and in Sec. 4 our results will be reported and discussed.

2 Theory

The fissioning transition nucleus is characterized by total angular momentum I and its projection on the spaced axis, M, and with its projection on the symmetry axis, K. If a compound state (I, M) fissions through a transition state K, the angular distribution is given by[5]

$$W^I_{M,K}(\theta) = \frac{(2I+1)}{4\pi}|d^I_{M,K}(\theta)|^2\,, \tag{1}$$

where the $d^I_{M,K}(\theta)$ functions are the rotational part of the collective wave function. Therefore, the fission fragment angular distribution offers a direct source of information on the spectrum of quantum states associated with the transmission nucleus. The K distribution of the levels in the transition nucleus for a given temperature is predicated to be Gaussian,

$$F(K) \propto \exp\bigl(-K^2/2K_0^2\bigr)\,, \tag{2}$$

and the variance of the K distribution (designated as K_0^2) is

$$K_0^2 = \Im_{\rm eff}\,T/\hbar^2\,. \tag{3}$$

The quantity $\Im_{\rm eff}$ is equal to $\Im_\perp\Im_{||}/(\Im_\perp - \Im_{||})$, where $\Im_\perp$ and $\Im_{||}$ are nuclear moments of inertia about an axis perpendicular and parallel to the symmetry axis, respectively, and T is the temperature of the nucleus at the saddle point.

If the target and projectile spins are zero, the angular distribution for a particular, I is

$$W(\theta) \propto \sum_{I=I_{\rm min}}^{I_{\rm max}} (2I+1)|d^I_{M=0,K}(\theta)|^2 \exp\Bigl[\frac{-K^2}{2K_0^2}\Big/\sum_{K=-I}^{I}\exp\Bigl(\frac{-K^2}{2K_0^2}\Bigr)\Bigr]\,. \tag{4}$$

When many I values of the compound nucleus contribute and the transmission coefficients T_l are known, the over all angular distribution for $M=0$ becomes[6]

$$W(\theta) \propto \sum_{I=I_{\rm min}}^{I_{\rm max}} (2I+1)T_I \sum_{K=-I}^{I}\Bigl\{(2I+1)|d^I_{M=0,K}(\theta)|^2 \exp\Bigl[\frac{-K^2}{2K_0^2}\Big/\sum_{K=-I}^{I}\exp\Bigl(\frac{-K^2}{2K_0^2}\Bigr)\Bigr]\Bigr\}\,, \tag{5}$$

where T_l is the transmission coefficients. If the target and projectile spins are included, an exact expression for the fission fragment angular distribution becomes[7]

$$W(\theta) = \sum_I \sum_{M=-(I_0+s)}^{(I_0+s)} \left[\sum_{j=|I_0-s|}^{I_0+s}\sum_{l=0}^{\infty}\sum_{\mu=-I_0}^{+I_0} \frac{1}{(2I_0+1)(2s+1)}\frac{(2l+1)T_l}{\sum_l(2l+1)T_l}|C^{I_0,s,j}_{\mu,M-\mu,M}|^2|C^{j,l,I}_{M,0,M}|^2\right]$$

$$\times \sum_{K=-I}^{I} \frac{(2I+1)|d^{I}_{M,K}(\theta)|^2 \exp(-K^2/2K_0^2)}{\sum_{K=-I}^{I} \exp(-K^2/2K_0^2)} . \quad (6)$$

the quantities I_0, s, and j are the target spin, projectile spin, and channel spin, respectively. The channel spin j is defined by the relation $j = I_0 \oplus s$. The total angular momentum I is given by the sum of the channel spin and orbit angular momentum, $I = j \oplus l$. The projection of I_0 on the space fixed axis is given by μ, whereas the projection of j (and I) on the space fixed axis is M. The quantity in the first set of large square brackets gives the weighting factor for a particular (I, M) combination. This value multiplies to angular-dependent term for the allowable K-state (K distribution is weighted also) of a particular I. This product is summed first over all M values for a particular I and finally over all I values.

3 Results and Discussions

The statistical variance K_0^2 has been deduced in the fission reaction ^{10}B + ^{232}Th, ^{10}B + ^{237}Np, ^{11}B + ^{237}Np, ^{12}C + ^{237}Np, and ^{16}O + ^{237}Np at typical energies. The analyses of experimental angular distribution of fission fragments at moderate excitation energies, which have been reported in the literature have been performed with Eqs. (5) and (6). The sharp cut-off approximations for optical model transmission coefficients are used in the calculations. The results for ^{10}B + ^{237}Np reaction at various bombarding energies are given in Table 1. It is clear that the values of K_0^2 calculated with expressions which do and do not include the projectile target spins are quite different.

Table 1 Variance K_0^2 obtained from theoretical calculations.

Reaction	$E_{\rm Lab}$ (MeV)	$K_0^{2\,\rm a}$	$K_0^{2\,\rm b}$	$\frac{W(\theta)}{W(90)}^{\rm c}$
^{10}B + ^{237}Np	70	207.36	150.03	1.57967
	64	190.44	141.24	1.34000
	60	132.25	112.89	1.32111
	56	122.89	95.347	1.14951
	53	110.25	88.486	1.09247

[a]Theoretical variance K_0^2, assuming zero projectile and target spin.
[b]Theoretical variance K_0^2, including the projectile and target spin.
[c]Experimental anisotropy.[8−11]

Full fission fragment angular distributions calculated by means of Eqs. (5) and (6) and by using the values of the variances K_0^2 from Table 1 are plotted in Figs. 1 and 2. From these figures, we see that statistical transition model gives generally a good agreement with experiment. However, their corresponding K_0^2 values are very different. In the figures the results of exact theoretical calculations with Eq. (6), which includes the spins of both target and projectile, are shown by solid curves. The results obtained with Eq. (5), which assumes that both the target and projectile spins are zero, are plotted as dashed curves. The values of K_0^2 derived from Eq. (5) is about 13% larger and demonstrates the error introduced by neglecting the target and projectile spins.

Table 2 Variance K_0^2 obtained from theoretical calculations.

Reaction	$E_{\rm Lab}$ (MeV)	$K_0^{2\,\rm a}$	$K_0^{2\,\rm b}$	$\frac{W(\theta)}{W(90)}^{\rm c}$
^{11}B + ^{237}Np	70	289.11	225.765	1.501 50
	60	169.05	135.874	1.342 99
	56	125.44	87.5437	1.146 59

[a]Variance K_0^2 from approximate theory, Eq. (5).
[b]Variance K_0^2 from exact theory, Eq. (6).
[c]Experimental anisotropy.[10,11]

The statistical variance K_0^2 obtained in the fission reaction ^{11}B+^{237}Np system at various bombarding energies is shown in Table 2. It is interesting to note that the K_0^2 values for this reaction is about 13% larger than the values deduced for ^{10}B+^{237}Np reaction. This clearly shows that the projectile spin also strongly influence the fragment anisotropies at near barrier energies. The full angular distributions calculated with exact theory, Eq. (6), and the approximate theory using the variances K_0^2 from Table 2 are plotted in Fig. 3. Although the general fits to the experimental data are equally good, however, the result obtained from the expression which includes the channel spin are much more superior.

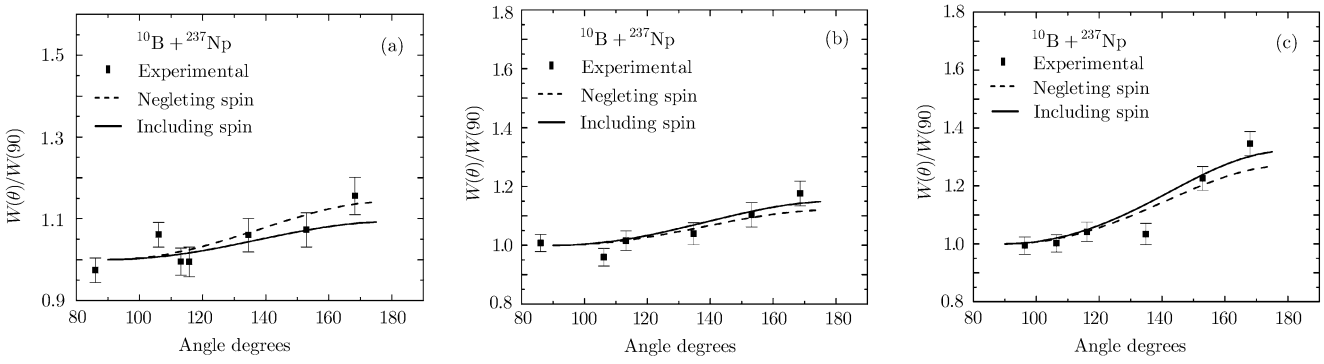

Fig. 1 Experimental fission fragment angular distributions of ^{10}B + ^{237}Np reaction at (a) $E_{\rm lab}$ = 53 MeV, (b) $E_{\rm lab}$ = 56 MeV, (c) $E_{\rm lab}$ = 60 MeV. The solid curves are for the exact theoretical calculation from Eq. (6). The dashed curves are the results from approximate Eq. (5).

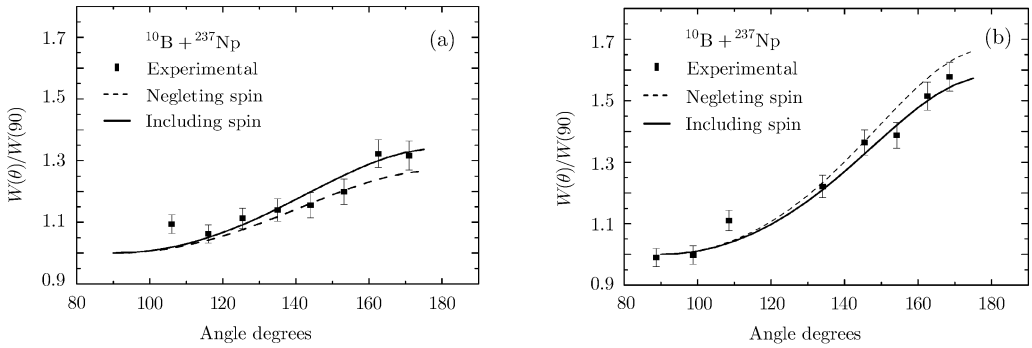

Fig. 2 The same as Fig. 1 but at (a) $E_{\rm lab} = 64$ MeV and (b) $E_{\rm lab} = 70$ MeV.

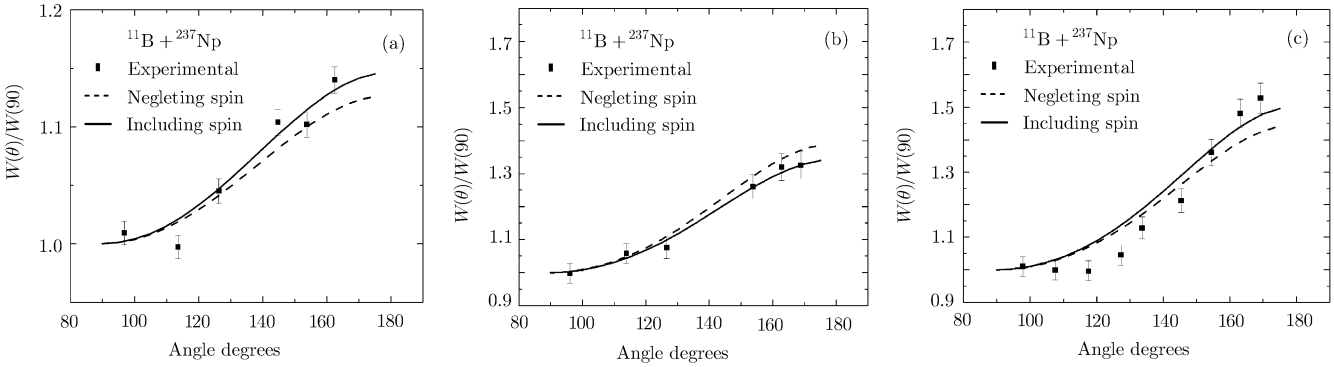

Fig. 3 Experimental fission fragment angular distributions of $^{11}B + ^{237}Np$ reaction for (a) $E_{\rm lab} = 56$ MeV, (b) $E_{\rm lab} = 60$ MeV, and (c) $E_{\rm lab} = 70$ MeV. The solid curves are the exact theoretical calculation by Eq. (6). The dashed curves are the results from approximate Eq. (5).

In some reactions the approximate theoretical expression deviates markedly from their corresponding experimental values. However, by considering entrance channel spin the agreement with experiment becomes very good. In Fig. 4 results of the exact theoretical angular distribution with Eq. (6) which includes the spins of both projectile and target are shown by solid curve. The results obtained with Eq. (5), which assumes both the target and projectile spins are zero, plotted as dashed curve. Comparing these with their corresponding experimental distributions it is seen that the results obtained with exact Eq. (6) is quite different, which demonstrates the influence of entrance channel spin on the angular anisotropies. This confirms that the presence of projectile target and ground state spins affects the fission fragment anisotropies in a significant way.

Several fission reactions are chosen to illustrate the dependence of the derived value of K_0^2 on the role of target spin on the theoretical analysis. The experimental fission anisotropies for the reactions ^{10}B and ^{12}C, on ^{232}Th and ^{237}Np are listed in Table 3. Their corresponding K_0^2 values deduced from the theoretical analysis are also listed in this table. The dada on Table 3 reveals clearly that the fragment anisotropy depends on target spin.

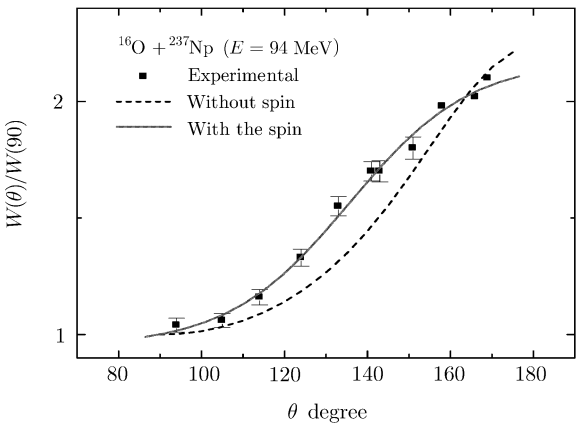

Fig. 4 Comparison of the experimental fission fragment angular distributions for $^{16}O + ^{237}Np$ reaction at 94 MeV. The approximate theoretical values are shown with a delta curve while the solid curve is the reaction obtained by considering the entrance chain spin.

To demonstrate the dependence of the variance K_0^2 on the values of the transmission coefficients appearing on the theatrical expressions (5) and (6), we have computed the variance K_0^2 for the $^{12}C + ^{209}Bi$ reaction in the same way as described above except that the values of the optical mode transmission coefficients were used instead. The results are displayed in Table 4. As can be seen from a comparison of these results, the neglection of the exact values of the transmission coefficients leads to a value of K_0^2, which is too large by several percent.

Table 3 Fission fragment anisotropies from different fission reactions.

Reaction	$E_{\rm Lab}$ (MeV)	$\frac{W(\theta)}{W(90)}$	K_0^2
$^{10}\mathrm{B} + ^{232}\mathrm{Th}$	68	1.572	161.88
$^{10}\mathrm{B} + ^{237}\mathrm{Np}$	68	1.335	226.76
$^{12}\mathrm{C} + ^{232}\mathrm{Th}$	77	1.667	192.23
$^{12}\mathrm{C} + ^{237}\mathrm{Np}$	77	1.450	233.75

Table 4 Variance K_0^2 obtained from theoretical calculations.

Reaction	E/V_B	Anisotropy	Variance K_0^2			
			a	b	c	d
$^{12}\mathrm{C} + ^{209}\mathrm{Bi}$	0.9	1.1	71.27	64.21	66.15	56.65
	1.03	1.4	87.03	73.14	78.71	63.66
	1.08	1.6	107.24	86.49	96.93	77.78
	1.25	2.05	157.87	127.69	142.12	113.43

[a]Calculated from Eq. (5) using the sharp cut-off approximation.

[b]Calculated from Eq. (5) using the actual values of the transmission coefficients.

[c]Calculated from Eq. (6) using the sharp cut-off approximation.

[d]Calculated from Eq. (6) using the actual values of the transmission coefficients.

4 Summary

In summary we have shown that the entrance channel dependence K-state model incorporating the ground state spins of the target and projectile explains the measured fragment anisotropies well for all systems under study. Our results further show that the variance K_0^2 calculated by considering the entrance channel spin are less than those calculated by neglecting the entrance channel spin which may imply the presence of reaction mechanisms such as channel coupling at those energies.

Acknowledgments

We acknowledge Mr. M. Gholami from Middle East Technical University, Ankara, Turkey, for his help in preparing the manuscript.

References

[1] A.N. Behkami and P. Nazar-Zadeh, J. Sci. I. R. Iran **9** (1998) 2.

[2] Bivash R. Behera, *et al.*, Phys. Rev. C **64** (2001) 041602.

[3] K. Mahata, S. Kailav, A Shrivastava, A. Chatterjec, P. Singh, and S. Santra, Phys. Rev. C. **65** 034613.

[4] R.G. Thomas, B.K. Nayak, A. Saxena, D.C. Biswas, L.M. Pant, and R.K. Choudury, Phys. Rev. C. **65** 057601.

[5] R. Vandenbosch and I.R.R. Huizenga, *Nuclear Fission*, Academis Press, New York (1973).

[6] A.N. Behkami, Z. Kargar, P. Nazar-Zadeh, and N. Azizi, NSJ **37(5)** (2002) 307.

[7] P. Nazar-Zadeh, Ph. D. Thesis, (1998).

[8] A. Shrivastava, *et al.*, Phys. Rev. Lett. **89** B (1999) 699.

[9] S. Kailas, Phys. Rev. **284** (1997) 381.

[10] N. Majumdar, *et al.*, Phys. Rev. Lett. **77** (1996) 5027.

[11] B.K. Nayak, *et al.*, Phys. Rev. C **64** (2000) 031601.